

Provided for non-commercial research and education use.  
Not for reproduction, distribution or commercial use.

ISBN 978-90-481-9817-7



NATO Science for Peace and Security Series - B:  
Physics and Biophysics

## Boron Rich Solids

Sensors, Ultra High Temperature  
Ceramics, Thermoelectrics, Armor

Edited by  
Nina Orlovskaya  
Mykola Lugovy

 Springer



This chapter was published in the above Springer book. The attached copy is furnished to the author for non-commercial research and education use, including for instruction at the author's institution, sharing with colleagues and providing to institution administration.

Other uses, including reproduction and distribution, or selling or licensing copies, or posting to personal, institutional or third party websites are prohibited.

In most cases authors are permitted to post their version of the chapter (e.g. in Word or TEX form) to their personal website or institutional repository.

## BORON UNDER PRESSURE: PHASE DIAGRAM AND NOVEL HIGH-PRESSURE PHASE

ARTEM R. OGANOV<sup>1,2,\*</sup>

<sup>1</sup> *Department of Geosciences, Department of Physics and Astronomy,  
and New York Center for Computational Sciences, Stony Brook  
University, Stony Brook, New York 11794-2100, USA*

<sup>2</sup> *Geology Department, Moscow State University, 119992 Moscow,  
Russia*

**Abstract** Boron has a unique chemistry, responsible for remarkable complexities even in the pure element. I review some of the history of the discovery of this element, and recent surprises found in boron under pressure. I discuss the recent discovery of a new high-pressure phase,  $\gamma$ -B<sub>28</sub>, consisting of icosahedral B<sub>12</sub> clusters and B<sub>2</sub> pairs in a NaCl-type arrangement: (B<sub>2</sub>)<sup>δ+</sup>(B<sub>12</sub>)<sup>δ-</sup>, and displaying a significant charge transfer  $\delta \sim 0.48$ . Boron is the only light element, for which the phase diagram has become clear only in the last couple of years, and this phase diagram is discussed here among other recent findings.

**Keywords:** boron allotropes, ab initio simulations, crystal structure prediction, phase diagram

### 1. Introduction

Boron can be called a frustrated element: situated between metals and insulators in the Periodic Table, it has only three valence electrons (favoring metallicity), but strongly localized<sup>1</sup> so that insulating states emerge at low pressures. Pressure, temperature and impurities easily shift this balance: for instance, while pure forms of boron are all semiconducting, doped boron is often metallic.

---

\* Department of Geosciences, Department of Physics and Astronomy, and New York Center for Computational Sciences, Stony Brook, University, Stony Brook, New York 11794-2100, USA. Geology Department, Moscow State University, 119992 Moscow, Russia, e-mail: [aoganov@notes.cc.sunysb.edu](mailto:aoganov@notes.cc.sunysb.edu)

<sup>1</sup> One parameter quantifying localization of valence electrons is their orbital radius; the outermost valence orbital radius for the boron atom is 0.78 Å, only slightly larger than that of carbon (0.62 Å), and much smaller than that of metals aluminum (1.31 Å) or gallium (1.25 Å).

At low pressures (<89 GPa) boron adopts structures based on icosahedral  $B_{12}$  clusters with metallic-like 3-centre bonds within the icosahedra and covalent 2-centre and 3-centre bonds between the icosahedra. Such bonding satisfies the octet rule and produces a delicate insulating state.

Among the reported phases of boron, probably only three correspond to the pure element [1, 2]: rhombohedral  $\alpha$ - $B_{12}$  and  $\beta$ - $B_{106}$  phases (with 12 and 106 atoms in the unit cell, respectively) and tetragonal T-192 (with 190-192 atoms/cell).

The high-pressure behaviour of boron is intriguing. On the one hand, pressure favours metallic states and might stabilise metallic-like icosahedral clusters [3]. On the other hand, packing efficiency of icosahedral structures is very low (34% for  $\alpha$ - $B_{12}$ , calculated assuming atomic radius equal to half the shortest B–B bond), necessitating the destruction of the icosahedra and formation of denser phases under pressure – e.g., the metallic  $\alpha$ -Ga-type phase [4, 5]. Metastable room-temperature compression of  $\beta$ - $B_{106}$  showed amorphization [3] at 100 GPa and the onset of superconductivity [6] at 160 GPa. The nature of the superconducting phase remained unclear, as did the phase diagram of boron, both at high and low pressures.

Before considering in greater detail the high-pressure behaviour of boron and the newly discovered  $\gamma$ - $B_{28}$  phase (subject of Section 3), we delve into the very instructive history of this element in the next section. Our review is based on our previous publications [7–9] and is intentionally non-technical (all the technical details interested readers can find in the original publications cited here).

## 2. A Bit of History

Boron is arguably the most complex element in the Periodic Table. The history of its studies is full of disputes, with mistakes made even by great scientists. At times this history may even read like a detective story.

A boron-containing mineral borax (probably from Persian “buraq”, meaning “white”),  $Na_2[B_4O_5(OH)_4] \cdot 8H_2O$ , was known since ancient times. In 1702, starting from borax, W. Homberg obtained a snow-white powder that he called “sedative salt”, now known as metaboric acid,  $HBO_2$ . The next stage, marked by the “double discovery” of this element, was at the time of scientific rivalry between great English (Humphry Davy) and French (Louis Joseph Gay-Lussac and Louis Jacques Thenard) chemists. On 21 June 1808, Gay-Lussac and Thenard announced the discovery of the new element, which they called “bore” (the element is still called this name in

French). They obtained boron by reduction of boric acid with potassium<sup>2</sup> [10]. Shortly afterwards, Humphry Davy submitted to the Royal Society of London an article on the discovery of a new element (which he called boracium)<sup>3</sup> [11]. Faithful to his style, which has led to the discovery of a whole pleiad of elements, Davy prepared boron by electrolysis. Curiously, both discoveries did not produce a pure element. It is now clear that both groups synthesized compounds containing not more than 50% of boron [12].

Henri Moissan, who proved that Gay-Lussac, Thenard and Davy did not deal with pure boron; in 1895 he prepared the element by reduction of  $B_2O_3$  with magnesium in a thermite-type reaction [12]. However, even Moissan's material was far being a pure element. It is often quoted that 99%-pure boron was synthesized by E. Weintraub [13] in 1909–1911, but there are reasons for doubt, as pure boron polymorphs are documented only after 1957.

After the element itself got more or less established, a saga of the discovery of boron polymorphs gradually began. And that saga was equally complex and full of misdiscoveries. Already in 1857 Friedrich Wöhler and Henri Sainte-Claire Deville [14, 15], heating up boron oxide and aluminium, obtained three forms of boron. On the basis of hardness and luster, they drew an analogy with carbon polymorphs and called these forms diamond-like, graphite-like and charcoal-like (amorphous). Amorphous form had the same properties as the material synthesized by Gay-Lussac and Thenard (which, as we now know, was not pure boron), while the “diamond-like” and “graphite-like” forms were later proven to be compounds containing not more than 70% of boron [12]. Thus, many, if not most, of the great scientists who studied boron, fell victims of this element's extreme sensitivity to even small amounts of impurities. This sensitivity is evidenced by the existence of such very boron-rich compounds (with unique icosahedral structures) as  $YB_{65.9}$ ,  $GeB_{90}$ ,  $B_6O$ ,  $NaB_{15}$ ,  $B_{12}P_2$ ,  $B_{13}P_2$ ,  $B_{13}C_2$ ,  $MgAlB_{14}$ ,  $AlC_4B_{40}$ ,  $B_{50}C_2$ ,  $B_{50}N_2$ ,  $PuB_{100(?)}$  (e.g., [1]). In particular, the structure of  $YB_{66}$  is an icon of structural complexity – it contains 1584 atoms in the unit cell [16].

At least 16 crystalline polymorphs have been described [1], but crystal structures were determined only for four modifications and most of the reported phases are likely to be boron-rich borides rather than pure elemental boron [1–3]. Until 2007, it was the only light element, for which the ground

<sup>2</sup> The story of how Gay-Lussac and Thénard obtained potassium is also quite instructive. Davy's discovery of this element by electrolysis caused a great excitement among chemists. Emperor Napoleon I, who awarded a prestigious prize to English chemist Humphry Davy, wished to foster similar kind of research (discovery of new elements by electrolysis) and presented Davy's competitors, Gay-Lussac and Thénard, with a very large electric battery. Disappointingly, the battery turned out to be not nearly as powerful as was expected. Gay-Lussac and Thénard, however, managed to prepare potassium (used for preparing boron) by heating up potash and iron.

<sup>3</sup> The material obtained by Davy appears to have been metallic, whereas pure boron phases are all semiconducting.

state was not known even at ambient conditions. And none of the polymorphs reported before 1957 actually correspond to pure boron. Most of the discoveries related to pure boron discoveries were done in two “waves” – 1957–1965 and 2001–2009.

The first wave was led by researchers from Cornell University and General Electric (GE) Corporation. The so-called I-tetragonal phase (or T-50, because it contains 50 atoms in the unit cell), produced in 1943 jointly at Cornell and GE [17], was the first one for which the structure was solved – in 1951 [18, 19]. However, this “well-established” phase was proven to be a compound [2, 20, 21] of composition  $B_{50}C_2$  or  $B_{50}N_2$ .

The first pure boron phase discovered was  $\beta$ - $B_{106}$  [22], the structure of which turned out to be extremely complex and was solved only several years later [23]. This discovery was shortly followed by the discoveries of  $\alpha$ - $B_{12}$  phase at GE in 1958 [24] and T-192 phase at Polytechnic Institute of Brooklyn in 1960 [25] (the structure of the latter was so complex that it was solved only in 1979 [26]). All these structures contain  $B_{12}$  icosahedra and are shown in Fig. 1.

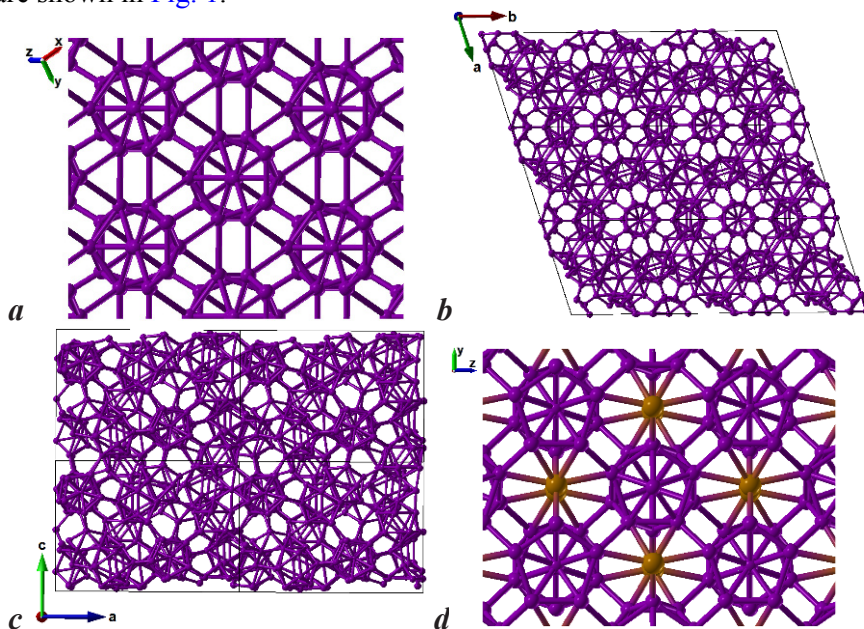


Figure 1. Crystal structures of boron polymorphs. (a)  $\alpha$ - $B_{12}$ , (b)  $\beta$ - $B_{106}$ , (c) T-192, (d)  $\gamma$ - $B_{28}$ . Panels (a) and (d) are from [1], (b) and (c) are from [7].

Because of the sensitivity of boron to impurities different samples of the same polymorph show important differences in structural and thermodynamic properties – as a result, the relative stability of boron phases is still experimentally unresolved even at ambient conditions [27]. It was, for

instance, a matter of a debate (until 2007) whether  $\alpha$ -B<sub>12</sub> or disordered  $\beta$ -B<sub>106</sub> is stable at ambient conditions. Amberger and Ploog [2] even suggested that only two known phases correspond to pure boron, namely,  $\alpha$ -B<sub>12</sub> and T-192, and possibly  $\beta$ -B<sub>106</sub>. They obtained boron by CVD using mixture of BBr<sub>3</sub> and H<sub>2</sub> at temperatures 1,200–1,600 K, with deposition on Ta wires in absence of any foreign atoms. This way they observed amorphous boron,  $\alpha$ -B<sub>12</sub> and T-192 phases, and occasionally  $\beta$ -B<sub>106</sub>.

As we mentioned, much of the progress was done at GE – at that time, GE amassed a unique group of researchers with the aim of enabling industrial-scale synthesis of diamond. Furthermore, GE researchers synthesized cubic BN, an advanced substitute for diamond in cutting and abrasive tools. Both synthetic diamond and cubic BN (commercialized under name “borazon”) turned into multimillion-dollar industries. GE was interested in boron, because of its extreme hardness and because of its highly tunable electrical conductivity. At least since the works of Sainte-Claire Deville and Wöhler in 1850s, boron was known to be the second hardest element after carbon (viz. diamond), and Weintraub [13] even entertained ideas that under certain fabrication protocol boron could become harder than black diamond (variety of diamond called “carbonado”)<sup>4</sup>.

Robert Wentorf of GE, one of the pioneers of high-pressure synthesis of materials and the main author of the synthesis of cubic BN, in 1965 explored the behavior of boron under pressure. At pressures above 10 GPa and temperatures 1,800–2,300 K, he found that both  $\beta$ -B<sub>106</sub> and amorphous boron transformed into another, hitherto unknown, phase [28]. Wentorf reported a qualitative diffraction pattern of the new material and described the changes of the density and electrical conductivity across the phase transition. Neither the chemical composition, nor structure or even lattice parameters were determined, however. For that time, it was a state-of-the-art work, but nevertheless it was not accepted by the community and Wentorf's diffraction data were deleted from Powder Diffraction Files Database. However, now it can be stated that with good likelihood Wentorf had synthesized phase now known as  $\gamma$ -B<sub>28</sub> [7] (probably in mixture with other phases).

The second wave of boron studies was probably catalyzed by the 2001 unexpected discovery of superconductivity in MgB<sub>2</sub> [29]. It is clear (e.g., [30]) that superconductivity comes from the boron sublattice of this structure, and that fuelled further research on pure boron. In 2001, compressing  $\beta$ -B<sub>106</sub>

<sup>4</sup> For example Weintraub wrote that “(pieces of boron) are very hard and scratch with ease the known hard substances except diamond”, “in further continuation of the work additional toughness may be imparted to boron and the product become a cheap substitute for black diamond” and “Will it be possible to approach the properties of diamond or perhaps by combining boron and carbon even exceed diamond in its hardness? I can only say that we are working on this problem.” [13]

at room temperature, Eremets et al. [6] indeed observed metallization at 160 GPa, and the metallic state displayed superconductivity (with the value of  $T_c$  reaching 11.2 K at 250 GPa). The structure of this metallic phase was not determined, but subsequent experiments [3] suggested that room-temperature compression of  $\beta$ -B<sub>106</sub> results in pressure-induced amorphization at 100 GPa. This implies that there is a kinetically hindered phase transition to some unknown crystalline phase below 100 GPa. Using laser heating to overcome kinetic barriers, Ma et al. [31] found that  $\beta$ -B<sub>106</sub> transforms into the T-192 phase above 10 GPa at 2,280 K. This proved that the T-192 phase is not only a pure boron phase, but also has a stability field at high pressures and temperatures. Its stability field was further constrained in [7].

At the same time, the stable phase at ambient conditions remained unknown. The debate whether  $\alpha$ -B<sub>12</sub> or  $\beta$ -B<sub>106</sub> is stable at ambient conditions was finally resolved in 2007–2009 by ab initio calculations of three different groups [32–34], which used different approaches, but all concluded in favor of  $\beta$ -B<sub>106</sub> and against common intuition that favored the much simpler  $\alpha$ -B<sub>12</sub> structure.

Another major result came from J. Chen and V.L. Solozhenko, who independently found a new phase of pure boron at pressures above 10–12 GPa and temperatures above 1,500 K. Further evolution of ideas and events completed the “second wave of boron research”, resolved many old problems and by itself could deserve a detective novel. This discovery is discussed in the following section.

### 3. Structure and Properties of a New Phase of Boron, $\gamma$ -B<sub>28</sub>

a. *Establishing the structure.* Although Chen managed to determine the unit cell parameters of the new phase (orthorhombic cell with  $a = 5.0544$  Å,  $b = 5.6199$  Å,  $c = 6.9873$  Å), neither he nor Solozhenko succeeded in solving its structure – in spite of intense research and repeated experiments during several years. In 2006, Chen posed this problem to me, with the idea that the method for predicting crystal structures [35] that I was developing at the time could be used for solving this problem. The structure (Fig. 1d) was solved within 1 day<sup>5</sup>.

USPEX [35] is an ab initio evolutionary algorithm, which searches for the structure with the lowest theoretical thermodynamic potential and requires no experimental information. However, the use of experimental cell parameters as constraints simplifies search and we took advantage of it.

<sup>5</sup> But it took much longer to publish these results. The paper was submitted to *Nature* on 27 January 2007 and it took 2 years to publish it in *Nature* (the paper came out on 28 January 2009). During this period, I learned about Solozhenko's independent work and our parallel teams merged.

From densities of other boron phases, we estimated the number of atoms in the cell to be between 24 and 32. Since this number has to be even to produce an insulating state, we considered cases of 24, 26, 28, 30 and 32 atoms/cell.

Figure 2 illustrates this search process by the sequence of lowest-energy structures in each generation for the 24-atom system. The first (random) generation did not contain any icosahedral structures. Increasingly large fragments of the icosahedra appear during calculation, until at the 11th generation the lowest-energy structure is found. Figure 3 shows the lowest-energy structures for each number of atoms in the unit cell. The 28-atom  $Pnnm$  structure (Fig. 1d) has the lowest energy per atom, correct orthorhombic

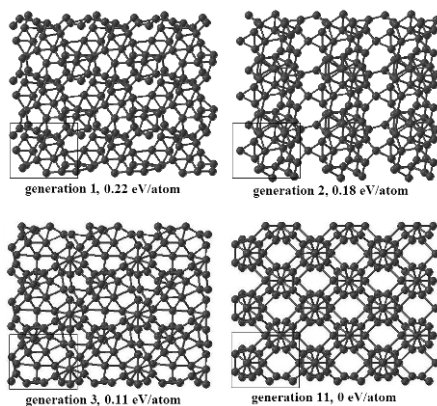


Figure 2. Example of an evolutionary simulation (24-atom system at fixed cell parameters). Best structure at each generation is shown (with total energies relative to the final energy) [7].

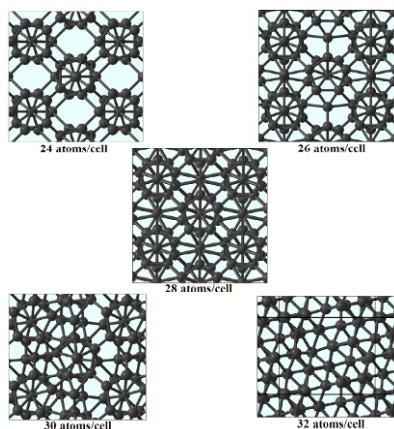


Figure 3. Best structures with 24, 26, 28, 30, 32 atoms/cell [7].



symmetry, and relaxed cell parameters and diffraction pattern in good agreement with experiment (Fig. 4). To make the test challenging and unbiased, it was done “blindly”, i.e. theoretical and experimental data were not exchanged until final comparison.

Table 1 gives predicted (at the DFT-GGA level of theory) structural parameters of  $\gamma$ -B<sub>28</sub> and two other stable boron phases with relatively simple structures (theoretical data on all structures are available from the author). Excellent agreement with available experimental data can be seen.

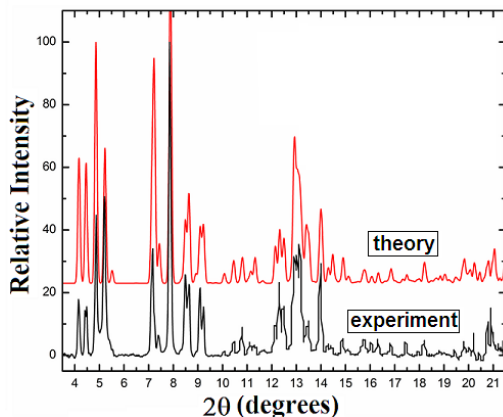


Figure 4. Comparison of theoretical and experimental X-ray powder diffraction profiles of  $\gamma$ -B<sub>28</sub>. X-ray wavelength  $\lambda = 0.31851 \text{ \AA}$  [7].

TABLE 1. Structures of stable boron phases (optimized at 1 atm), with Bader charges (Q) and volumes (V). Experimental data are in parentheses (Refs.7, 36). Atomic volumes are given in atomic units (a.u. = 1 bohr<sup>3</sup>). From [7]

Wyckoff position	x	y	z	Q <sub>PAW</sub>	Q <sub>LCAO-QZ</sub>	Q <sub>IAM</sub>	V <sub>LCAO-QZ</sub> , a.u.	V <sub>IAM</sub> , a.u.
$\gamma$ -B <sub>28</sub> . Space group <i>Pnnm</i> . $a = 5.043$ (5.054) $\text{\AA}$ , $b = 5.612$ (5.620) $\text{\AA}$ , $c = 6.921$ (6.987) $\text{\AA}$								
B1 (4g)	0.1702	0.5206	0	+0.2418	+0.1704	+0.0250	47.65	49.94
B2 (8h)	0.1606	0.2810	0.3743	-0.1680	-0.1430	-0.0153	48.46	46.25
B3 (8h)	0.3472	0.0924	0.2093	+0.0029	+0.0218	+0.0035	47.17	46.90
B4 (4g)	0.3520	0.2711	0	+0.0636	+0.0301	-0.0003	44.93	46.40
B5 (4g)	0.1644	0.0080	0	+0.0255	+0.0419	-0.0011	46.38	47.60
$\alpha$ -B <sub>12</sub> . Space group $R\bar{3}m$ . $a = b = c = 5.051$ (5.064) $\text{\AA}$ , $\alpha = \beta = \gamma = 58.04$ (58.10) $^\circ$ .								
B1 (18h)	0.0103	0.0103	0.6540	+0.0565	+0.0416	-0.0030	47.64	49.05
	(0.0102)	(0.0102)	(0.6536)					
B2 (18h)	0.2211	0.2211	0.6305	-0.0565	-0.0416	+0.0030	50.43	49.01
	(0.2212)	(0.2212)	(0.6306)					
$\alpha$ -Ga structure. Space group <i>Cmca</i> . $a = 2.939$ $\text{\AA}$ , $b = 5.330$ $\text{\AA}$ , $c = 3.260$ $\text{\AA}$ .								
B1 (8f)	0	0.1558	0.0899	0	0	0	43.08	43.08

Figure 5 shows results of *ab initio* calculations of relative stability of different phases of boron. As expected, the impurity-stabilized T-50 phase is energetically poor, while  $\alpha$ -B<sub>12</sub>,  $\beta$ -B<sub>106</sub>, T-192 and  $\gamma$ -B<sub>28</sub> phases are energetically nearly degenerate at low pressures.

According to these calculations,  $\gamma$ -B<sub>28</sub> is energetically more favorable than any known or hypothetical phase of boron at pressures between 19 and 89 GPa. At these conditions, it is also dynamically stable, i.e does not have any imaginary phonon frequencies (Fig. 6).

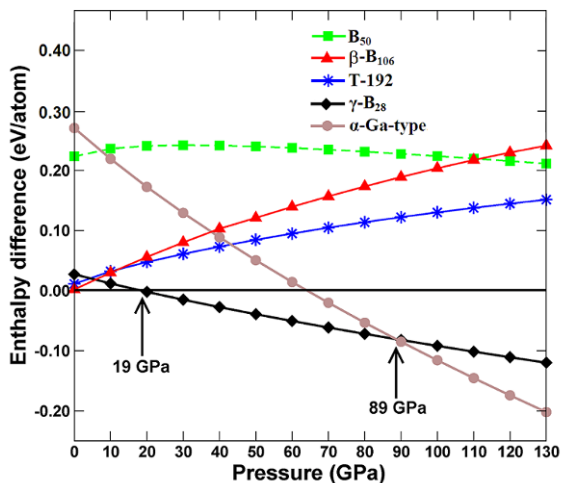


Figure 5. Stability of boron phases at 0 K. Enthalpies are shown relative to  $\alpha$ -B<sub>12</sub>. Phase transformations occur at 19 GPa ( $\alpha$ -B<sub>12</sub> to  $\gamma$ -B<sub>28</sub>) and 89 GPa ( $\gamma$ -B<sub>28</sub> to  $\alpha$ -Ga-type). From [7].

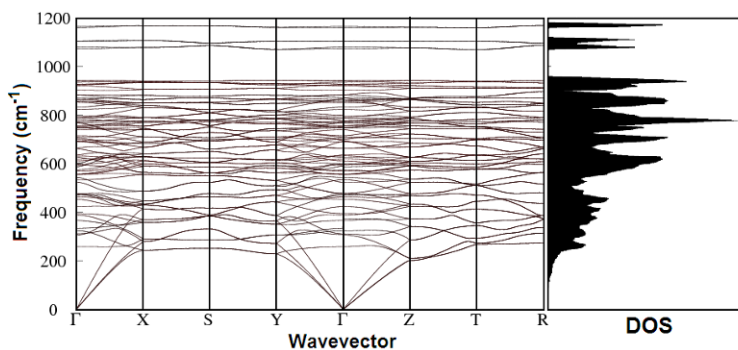


Figure 6. Theoretical phonon dispersion curves and phonon density of states of  $\gamma$ -B<sub>28</sub> at 1 atm. From [7].

b. *Chemical bonding and physical properties of the new phase.* The  $\gamma$ - $B_{28}$  structure is quite unique: centres of the  $B_{12}$  icosahedra (formed by sites  $B_2$ – $B_5$  – Table 1) form a slightly distorted cubic close packing (as in  $\alpha$ - $B_{12}$ ), in which all octahedral voids are occupied by  $B_2$  pairs (formed by site  $B_1$ ). It can be represented as a NaCl-type structure, the roles of “anion” and “cation” being played by the  $B_{12}$  icosahedra and  $B_2$  pairs, respectively.  $\gamma$ - $B_{28}$  is structurally similar to  $\alpha$ - $B_{12}$ , but denser due to the presence of additional  $B_2$  pairs. The average intraicosahedral bond length is 1.80 Å and the B–B bond length within the  $B_2$  pairs is 1.73 Å.

$\gamma$ - $B_{28}$  is the densest, and the hardest, of all known boron phases (all of which are superhard). The best estimates of the hardness of  $\beta$ - $B_{106}$  and  $\alpha$ - $B_{12}$  are 45 GPa [37] and 42 GPa [38], respectively, whereas for  $\gamma$ - $B_{28}$  the measured Vickers hardness of this phase is 50 GPa [8], which puts it among half a dozen hardest materials known to date. The high density of this phase is due to the close packing of the  $B_{12}$  icosahedra (like in  $\alpha$ - $B_{12}$ , the second densest known phase), where the “empty” space is filled by the  $B_2$  pairs.

Detailed investigations showed that the two clusters have very different electronic properties and there is charge transfer (of  $\sim 0.5$  e) from  $B_2$  to  $B_{12}$  (Fig. 7) [7], and this is correlated with the strong IR absorption and large dynamical charges on atoms.

$\gamma$ - $B_{28}$  is structurally related to several well-known compounds – for instance,  $B_6P$  or  $B_{13}C_2$ , where the two sublattices are occupied by different chemical species (instead of interstitial  $B_2$  pairs there are P atoms or C–B–C groups, respectively). This fact again highlights the chemical difference between the two constituent clusters. One can call  $\gamma$ - $B_{28}$  a “boron boride”  $(B_2)^{\delta+}(B_{12})^{\delta-}$  with partial charge transfer  $\delta$ .

While broken-symmetry structures, with two sublattices of the same element in different chemical roles, are known for some metals (e.g. Rb and Ba under pressure [39]),  $\gamma$ - $B_{28}$  is different: it is non-metallic, its two sublattices are occupied not by single atoms but by clusters ( $B_{12}$  and  $B_2$ ). The exact values of the atomic charges are definition-dependent, but qualitatively consistent:  $\delta \sim +0.2$  from differences in the numbers of electrons within atom-centred spheres (sphere radii 0.7–1.0 Å); Born dynamical charges attain much higher values (spherically averaged  $\delta = +2.2$ ). Our preferred estimates of CT are based on Bader theory [40], which partitions the total electron density (ED) distribution into “atomic” regions separated by zero-flux (i.e. minimum-density) surfaces, and give  $\delta = +0.48$  (Table 1). Bader partitioning is physically unbiased and ensures maximum additivity and transferability of atomic properties [40].

These relatively large Bader charges originate from the interaction between the  $B_2$  and  $B_{12}$  clusters: the Independent Atom Model (IAM, where the total ED is a sum of atomic densities) has negligible charges, an order of

magnitude lower than when the atoms are allowed to interact. Removing the  $B_2$  pairs from the structure, we again obtain negligible charges (within  $\pm 0.03$ ) even in the interacting system. The bond asymmetry parameter for this partially “ionic” bond reaches 20%. Because of CT, atomic volumes overall shrink (relative to the IAM) for positively charged and expand for negatively charged atoms (Table 1).

Figure 7 shows the total and local electronic densities of states; it can be seen that there are large differences in local DOSs of the  $B_2$  and  $B_{12}$  clusters in the bottom of the valence band ( $B_{12}$ -dominated), top of the valence band and bottom of the conduction band ( $B_2$ -dominated). While this is consistent with significant charge transfer  $B_2 \rightarrow B_{12}$ , there is also a strong covalency in the system seen from strong hybridization in the middle of the valence band.

Additional insight is provided by energy-decomposed electron density distribution (Fig. 8). Again, it is clear (even clearer than on Fig. 7) that lowest-energy valence electrons are concentrated around the  $B_{12}$  icosahedra, while HOMO and LUMO levels are  $B_2$ -dominated.

Ionicity affects many properties of  $\gamma$ - $B_{28}$ : high-frequency ( $\epsilon_\infty$ ) and static ( $\epsilon_0$ ) dielectric constants are very different (11.4 and 13.2, respectively), implying the LO-TO splitting as in ionic crystals, and strong infrared (IR) absorption. Being extremely sensitive to crystal structure and to the approximations of theory, the IR spectrum provides a very stringent test. The computed and measured (in the range 100–1,200  $\text{cm}^{-1}$ ) IR spectra show good agreement [7].

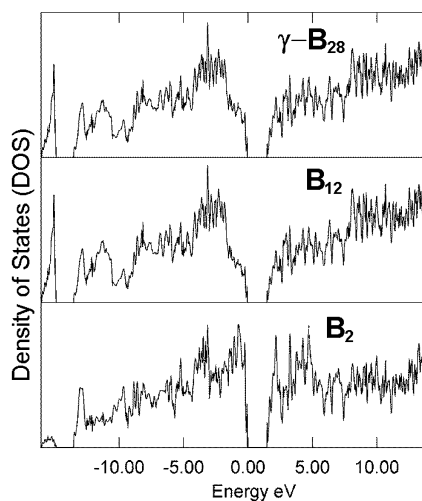


Figure 7. Total electronic density of states of  $\gamma$ -boron and its projections (per atom) onto  $B_{12}$  icosahedra and  $B_2$  pairs.

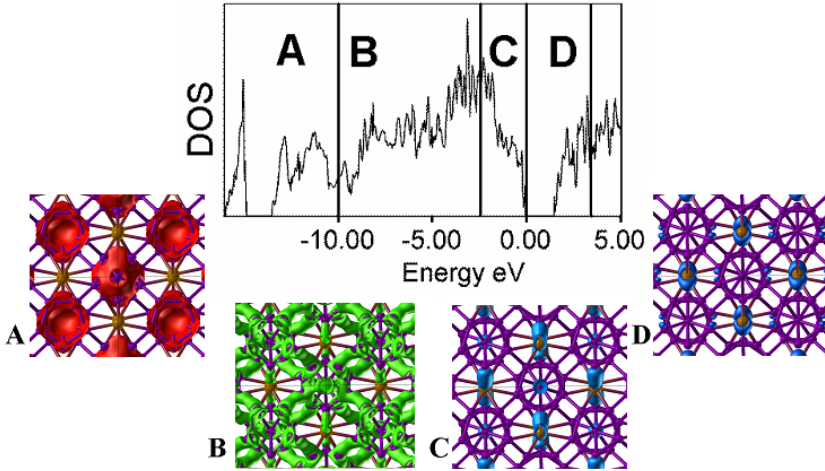


Figure 8. Electronic structure of  $\gamma$ -B<sub>28</sub>. The total density of states is shown, together with the electron density corresponding to four different energy regions denoted by letters A, B, C, D. Note that lowest-energy electrons are preferentially localized around the B<sub>12</sub> icosahedra, whereas highest-energy electrons (including the bottom of the conduction band – “holes”) are concentrated near the B<sub>2</sub> pairs. The fact that lowest-energy electrons belong to the B<sub>12</sub> clusters, and highest-energy – to B<sub>2</sub> units, is consistent with the direction of charge transfer: B<sub>2</sub> → B<sub>12</sub>. From [9].

The LO-TO splitting is different for all modes and reciprocal-space directions, and the simplest parameter characterising it is  $\zeta = \prod_{i=1}^n \left( \frac{\omega_i^{LO}}{\omega_i^{TO}} \right)^2 = \frac{\epsilon_0}{\epsilon_\infty}$ .  $\zeta=1$  for non-ionic crystals (the computed value is 1.01 for  $\alpha$ -B<sub>12</sub>) and  $\zeta > 1$  whenever there is CT (1.16 for  $\gamma$ -B<sub>28</sub> and 1.18 for GaAs). Individual mode splittings tend to be smaller for more complex structures, and the largest splitting in  $\gamma$ -B<sub>28</sub> (337–375 cm<sup>-1</sup>) occurs for the most intense IR-active mode, a nearly rigid-body anti-phase motion of the B<sub>2</sub> and B<sub>12</sub> units. Despite structural relationship with  $\alpha$ -B<sub>12</sub> (Fig. 1), the electronic structure of partially ionic  $\gamma$ -B<sub>28</sub> is quite different: it shows little pressure dependence of the band gap and even at 200 GPa remains an insulator with a relatively wide gap (1.25 eV – and one has to bear in mind that DFT band gaps are usually ~40% underestimated), whereas for the covalent  $\alpha$ -B<sub>12</sub> the calculated band gap rapidly decreases on compression and closes at ~160 GPa (Fig. 9). The key for this different behaviour is CT.

The example of  $\gamma$ -B<sub>28</sub> shows that significant ionicity can occur in elemental solids – though similar suggestions (e.g. hydrogen with H<sup>+</sup>H<sup>-</sup> molecules [41]) existed before. The key is the ability of boron to form clusters with very different electronic properties. The cationic B<sub>2</sub><sup>4+</sup> group is

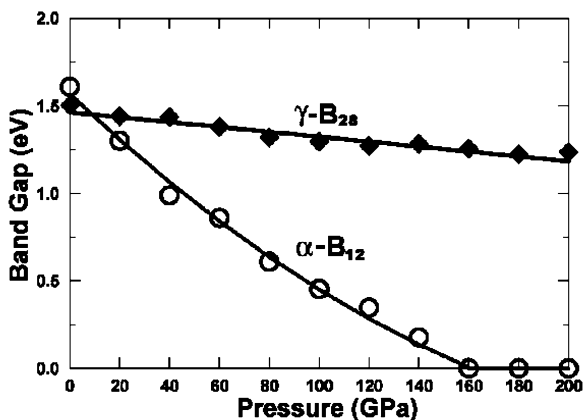


Figure 9. Pressure dependence of the band gap of  $\alpha\text{-B}_{12}$  and  $\gamma\text{-B}_{28}$ . From [7].

well known and its typical B–B distance [42] (1.70–1.75 Å in  $\text{B}_2\text{F}_4$  and  $\text{B}_2\text{Cl}_4$ ) is the same as in  $\gamma\text{-B}_{28}$  (1.73 Å). The  $\text{B}_{12}$  cluster is more stable as the  $\text{B}_{12}^{2-}$  anion (as in the very stable icosahedral  $(\text{B}_{12}\text{H}_{12})^{2-}$  cluster [42]), because in the neutral state it has an unoccupied bonding orbital (e.g., [43]). This orbital creates an acceptor band above the valence band edge in boron-rich solids. Electrons from dopant metal atoms or from other boron clusters may partially occupy this band, as detected by optical spectroscopy [44]. The  $\text{B}_2$  pairs thus behave as electron donors, similar to the metal dopants in boron-rich borides.

Significant charge transfer can be found in other elemental solids, and observations of dielectric dispersion [45], equivalent to LO-TO splitting, suggest it for  $\beta\text{-B}_{106}$ . The nature of the effect is possibly similar to  $\gamma\text{-B}_{28}$ . Detailed microscopic understanding of charge transfer in  $\beta\text{-B}_{106}$  would require detailed knowledge of its structure, and reliable structural models of  $\beta\text{-B}_{106}$  finally begin to emerge from computational studies [32–34].

One should realize that ionicity can appear in elements only as a result of many-body interactions, which are strongest under pressure or when atomic orbitals are diffuse (but not diffuse enough to form metallic states) – i.e. at the border between metallic and insulating states. Amphoteric elements close to the Zintl line (B–Si–As–Te–At) are particularly favorable. Solids made of nanoclusters with very different electronic structures can be significantly ionic; and short-lived ionic species may exist in elemental fluids.

c. *Phase diagram of boron.* The discovery of  $\gamma\text{-B}_{28}$  provided the missing piece of the puzzle of phase diagram of boron [7]. The stability field of this phase is larger than the fields of all other known boron polymorphs combined (Fig. 11). The diagram shown in Fig. 11 describes all known data in a consistent manner. The upper pressure limit of stability of  $\gamma\text{-B}_{28}$  remains to be tested. Theoretical predictions of an  $\alpha\text{-Ga}$ -type metallic phase above 74

GPa [4, 5] were confirmed [7] using crystal structure prediction tools [35], except that the predicted pressure of this phase transition was shifted to a higher value, 89 GPa, by the presence of a new phase,  $\gamma$ -B<sub>28</sub> [7].  $\alpha$ -Ga-type boron has been predicted to be a superconductor [46]. It has been found in our fully unconstrained variable-cell evolutionary simulations at 100 and 300 GPa. This structure does not contain B<sub>12</sub> icosahedra and heralds a new type of boron chemistry under pressure (Fig. 10).

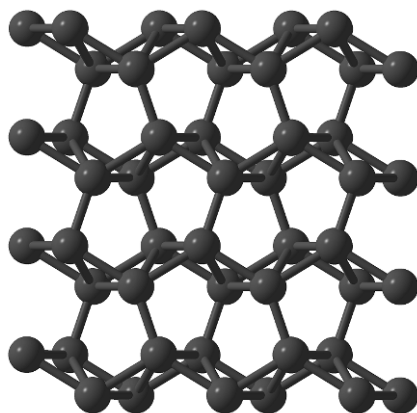


Figure 10.  $\alpha$ -Ga-type structure found in evolutionary simulations at 100 and 300 GPa.

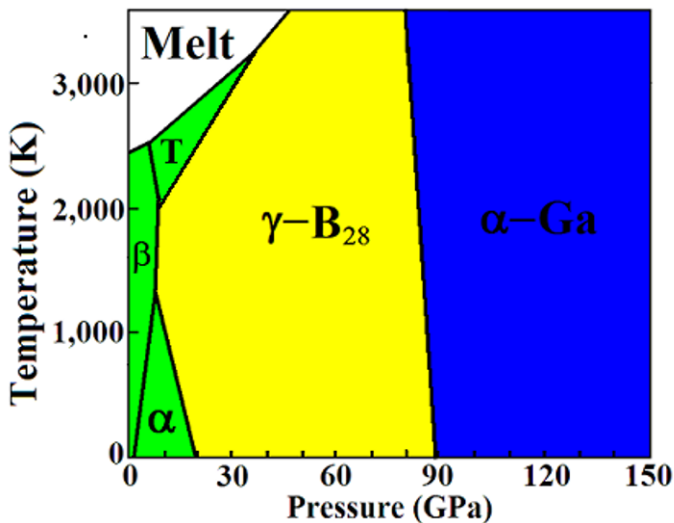


Figure 11. Phase diagram of boron. Reproduced from [7]. This schematic diagram is based on theoretical and experimental results from [7] and previous experimental [31, 47] and theoretical [32, 33] studies. The phase boundary between  $\gamma$ -B<sub>28</sub> and  $\alpha$ -Ga-type phases is based on the static transition pressure (89 GPa) and a Clapeyron slope of  $-2.71$  MPa/K calculated using density-functional perturbation theory and the GGA level of theory ( $-2.52$  MPa/K using the LDA). The calculated Clapeyron slope for the  $\alpha$ - $\gamma$  transition is  $-4.7$  MPaK<sup>-1</sup>.

d. *Subsequent works.* The equation of state of  $\gamma$ -B<sub>28</sub> was experimentally determined by Le Godec et al. [48] and is in excellent agreement with theoretical calculations of [7]. Very recently, Zarechnaya et al. [49, 50] experimentally confirmed the structure [7] and superhardness [8] of  $\gamma$ -B<sub>28</sub>, and also presented some calculations. Their main achievement was the synthesis of micron-sized single crystals and single-crystal confirmation of the structure, but unfortunately conditions of synthesis were suboptimal (e.g., the capsules reacted with boron sample), and their papers contained many errors [52]. For instance, their estimated density differences between boron allotropes were wrong by an order of magnitude (they claimed that  $\gamma$ -B<sub>28</sub> is 1% denser than all other forms of boron, while it is actually 8.3% denser than  $\beta$ -B<sub>106</sub>), which is possibly a result of incorrectly performed ab initio calculations in their papers. Their equation of state, measured to 30 GPa [49], shows large discrepancies with theory [7, 51] and earlier more careful experiment [48], see Fig. 12. Jiang et al. [51] computed the equation of state, the elastic constants (from which they obtained the bulk modulus of 224 GPa and shear modulus of 236 GPa, whereas the experimental bulk modulus is 238 GPa [48]), and remarkably high ideal tensile strengths (65, 51, and 52 GPa along the three crystallographic axes - similar to the measured hardness of 50 GPa [8]). They found that during deformation of the structure, the first bonds to break are those between the most charged atomic positions [51]. Other calculations showed that the electronic spectra of the different atomic sites in  $\gamma$ -B<sub>28</sub> are indeed very different [53], confirming

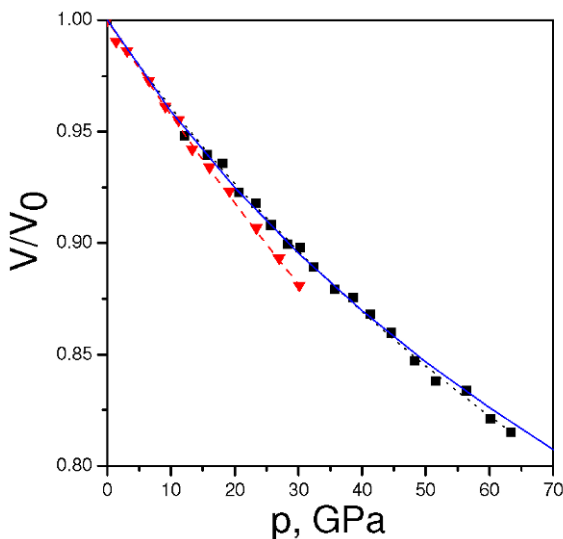


Figure 12. Equation of state of  $\gamma$ -B<sub>28</sub>: red triangles – experiment [49] (dashed line – Vinet fit), black squares – more careful experiment [48] (dotted line – Vinet fit), solid line – ab initio results [7]. Figure courtesy V.L. Solozhenko and O.O. Kurakevych, from [52].



the charge-transfer model of [7]. Furthermore, charge transfer seems to be required in this structure, which violates the “covalent” Wade-Jemmis electron counting rules [53]. A summary of work on this phase is given in Table 2.

TABLE 2. Summary of work on  $\gamma$ -B<sub>28</sub> phase

Reference	Main findings	Submission date
Wentorf [28]	Synthesis, density measurement, qualitative X-ray diffraction, electrical conductivity change across $\beta$ - $\gamma$ transition. No chemical analysis and no structure determination.	04.10.1964
Oganov et al. [7]	Synthesis and proof of chemical purity, structure determination, demonstration of partial ionicity, phase diagram.	27.01.2007
Solozhenko et al. [8]	Hardness measurement.	03.10.2008
Zarechnaya et al. [50,52]	Confirmation of synthesis and structure. Identified $\gamma$ -B <sub>28</sub> with Wentorf's phase.	03.11.2008
Le Godec et al. [48]	Accurate measurement of the equation of state at 300 K.	08.01.2009
Zarechnaya et al. [49,52]	Re-confirmation of structure using single crystals. Measurements of the band gap and electrical conductivity. Inaccurate measurements of the equation of state and hardness at 300 K. Incorrect interpretations of chemical bonding and density differences in boron allotropes.	16.01.2009
Jiang et al. [51]	Simulation of structure deformation.	12.03.2009
Rulis et al. [52]	Simulation of electronic spectra, supporting charge transfer picture.	06.04.2009

#### 4. Conclusions, and What Happens at Still Higher Pressures?

Boron is still an element of surprise, and many aspects of its behavior remain enigmatic. What happens beyond the stability field of  $\gamma$ -B<sub>28</sub>? We know that at room temperature  $\beta$ -B<sub>106</sub> amorphizes at  $\sim$ 100 GPa [3], but all this really means is that before 100 GPa  $\beta$ -B<sub>106</sub> becomes less stable than some other crystalline form, the transition to which is kinetically hindered at 298 K. In the absence of thermodynamically equilibrated experiments, there are several theoretical results, based on educated guesses [4, 5] of high-pressure structures, and on evolutionary crystal structure prediction

[35] – all consistently pointing to the  $\alpha$ -Ga-type phase, which has also been predicted [46] to be superconducting. Its structure does not contain any  $B_{12}$  icosahedra and heralds an entirely new chemistry for boron. However, due to the strongly localized nature of boron's valence electrons, this phase is only a poor metal, strongly deviating from free-electron behavior. This is reflected in its peculiar structure, which contains B–B pairs. In a sense,  $\gamma$ - $B_{28}$ , discovered in [7] and containing both the  $B_{12}$  icosahedra and  $B_2$  pairs, is a step between low-pressure icosahedral structures and the very high-pressure  $\alpha$ -Ga structure, which contains only  $B_2$  pairs and is entirely devoid of the icosahedra. Considering all these structural changes, one may conclude that boron chemistry becomes simpler with pressure – thus, high-pressure studies may actually lead to better understanding of low-pressure phenomena, affecting the entire field of boron chemistry. A very exciting field indeed.

## Acknowledgments

This chapter is a theoretician's overview of our recent results [7–9] (to which we refer the reader for more details, in particular, about the computational methodology and experimental data) and the related works, and I express deepest gratitude to my collaborators. To Jihua Chen for attracting me to the study of boron and, to Vladimir L. Solozhenko for his deep insight and warm friendship, to Carlo Gatti for sharing his exceptional chemical intuition and friendship.

## References

1. Douglas, B.E., Ho, S.-M., *Structure and Chemistry of Crystalline Solids* (Springer, N.Y., 2006).
2. Amberger, E., Ploog, K. (1971). Bildung der Gitter des Reinen Bors. *J. Less-Common Metals* **23**, 21–31.
3. Sanz D.N., Loubeyre P., Mezouar M. (2002). Equation of state and pressure induced amorphization of beta-boron from X-ray measurements up to 100 GPa. *Phys. Rev. Lett.* **89**, 245501.
4. Segall D.E., Arias T.A. (2003). Ab initio approach for high-pressure systems with application to high-pressure phases of boron: Perturbative momentum-space potentials. *Phys. Rev.* **B67**, 064105.
5. Haussermann U., Simak S.I., Ahuja R., Johansson B. (2003). Metal-nonmetal transition in the boron group elements. *Phys. Rev. Lett.*, **90**, 065701.
6. Eremets M.I., Struzhkin V.W., Mao H.K., Hemley R.J. (2001). Superconductivity in boron. *Science* **293**, 272–274.
7. Oganov A.R., Chen J., Gatti C., Ma Y.-M., Yu T., Liu Z., Glass C.W., Ma Y.-Z., Kurakevych O.O., Solozhenko V.L. (2009). Ionic high-pressure form of elemental boron. *Nature* **457**, 863–867.

8. Solozhenko V.L., Kurakevych O.O., Oganov A.R. (2008). On the hardness of a new boron phase, orthorhombic  $\gamma$ -B<sub>28</sub>. *J. Superhard Mater.* **30**, 428–429.
9. Oganov A.R., Solozhenko V.L. (2009). Boron: a hunt for superhard polymorphs. *J. Superhard Materials* **31**, 285–291.
10. Gay-Lussac J.L., Thenard L.J. (1808). Sur la décomposition et la recombinaison de l'acide boracique. *Ann. Chim. Phys.* **68**, 169–174.
11. Davy H. (1808). Electro-Chemical Researches, on the Decomposition of the Earths; With Observations on the Metals Obtained from the Alkaline Earths, and on the Amalgam Procured from Ammonia (Read June 30, 1808) *Phil. Trans. R. Soc. Lond.* **98**, 333–370.
12. Moissan H. (1895). Etude du Bore Amorphe. *Ann. Chim. Phys.* **6**, 296–320.
13. Weintraub E. (1911). On the properties and preparation of the element boron. *J. Ind. Eng. Chem.*, **3**(5), 299–301.
14. Sainte-Claire Deville H., Wöhler F. (1857). Ueber das Bor. *Ann. Physik* **100**, 635–646.
15. Wöhler F., Sainte-Claire Deville H. (1858). Du Bore. *Ann. Chim. Phys.* **52**(3), 63–92.
16. Richards S.M., Kasper J.S. (1969). The crystal structure of YB<sub>66</sub>. *Acta Cryst.* **B25**, 237–251.
17. Laubengayer A.W., Hurd D.T., Newkirk A.E., Hoard J.L. (1943). Boron. I. Preparation and properties of pure crystalline boron. *J. Am. Chem. Soc.*, **65**, 1924–1931.
18. Hoard J.L., Geller S., Hughes R.E. (1951). On the structure of elementary boron. *J. Am. Chem. Soc.*, **73**, 1892–1893.
19. Hoard J.L., Hughes R.E., Sands D.E. (1958). The structure of tetragonal boron. *J. Am. Chem. Soc.*, **80**, 4507–4515.
20. Will G., Ploog K. (1974). Crystal structure of I-tetragonal boron. *Nature* **251**, 406–408.
21. Ploog K., Amberger E. (1971). Kohlenstoff-Induzierte Gitter beim Bor: I-Tetragonales (B<sub>12</sub>)<sub>4</sub>B<sub>2</sub>C und (B<sub>12</sub>)<sub>4</sub>B<sub>2</sub>C<sub>2</sub>. *J. Less-Comm. Metals* **23**, 33–42.
22. Sands D.E., Hoard J.L. (1957). Rhombohedral elemental boron. *J. Am. Chem. Soc.*, **79**, 5582–5583.
23. Hughes R.E., Kennard C.H.L., Sullenger D.B., Weakliem H.A., Sands D.E., Hoard J.L. (1963). The structure of  $\beta$ -rhombohedral boron. *J. Am. Chem. Soc.*, **85**, 361–362.
24. McCarty L.V., Kasper J.S., Horn F.H., Decker B.F., Newkirk A.F. (1958). A new crystalline modification of boron. *J. Am. Chem. Soc.*, **80**, 2592.
25. Talley C.P. (1960). A new polymorph of boron. *Acta Cryst.*, **13**, 271–272.
26. Vlasse M., Naslain R., Kasper J.S., Ploog K. (1979). Crystal structure of tetragonal boron related to  $\alpha$ -AlB<sub>12</sub>. *J. Sol. State Chem.*, **28**, 289–301.
27. Chase M.W., Jr. (1998). *NIST-JANAF Thermochemical Tables*. Fourth Edition. J. Phys. Chem. Ref. Data Monograph No. 9. American Chemical Society, American Institute of Physics, National Institute of Standards and Technology. 1951 p.
28. Wentorf, R. H., Jr. (1965). Boron: another form. *Science* **147**, 49–50.
29. Nagamatsu J., Nakagawa N., Muranaka T., Zenitani Y. & Akimitsu J. (2001) Superconductivity at 39 K in magnesium diboride. *Nature* **410**, 63–64.
30. Ma Y., Wang Y., Oganov A.R. (2009). Absence of superconductivity in the novel high-pressure polymorph of MgB<sub>2</sub>. *Phys. Rev.* **B79**, 054101.
31. Ma Y.Z., Prewitt C.T., Zou G.T., Mao H.K., Hemley R.J. (2003). High-pressure high-temperature x-ray diffraction of beta-boron to 30 GPa. *Phys. Rev.* **B67**, 174116.
32. van Setten M.J., Uijtewaald M.A., de Wijs G.A., de Groot R.A. (2007). Thermodynamic stability of boron: The role of defects and zero point motion. *J. Am. Chem. Soc.* **129**, 2458–2465.
33. Widom M., Mikhalkovic M. (2008). Symmetry-broken crystal structure of elemental boron at low temperature. *Phys. Rev.* **B77**, 064113.

34. Ogitsu T., Gygi F., Reed J., Motome Y., Schwegler E., Galli G. (2009). Imperfect crystal and unusual semiconductor: Boron, a frustrated element. *J. Am. Chem. Soc.* **131**, 1903–1909.
35. Oganov A.R., Glass C.W. (2006). Crystal structure prediction using *ab initio* evolutionary techniques: principles and applications. *J. Chem. Phys.* **124**, 244704.
36. Will G., Kiefer B. (2001). Electron deformation density in alpha-boron. *Z. Anorg. Allg. Chem.* **627**, 2100–2104.
37. Gabunia D., Tsgareishvili O., Darsavelidze G., Lezhava G., Antadze M., and Gabunia L. (2004). Preparation, structure and some properties of boron crystals with different content of  $^{10}\text{B}$  and  $^{11}\text{B}$  isotopes. *J. Solid State Chem.* **177**, 600–604.
38. Amberger E., Stumpf W. (1981). *Gmelin Handbook of Inorganic Chemistry*, Springer-Verlag: Berlin. 1960, pp. 112–238.
39. McMahan M.I., Nelmes R.J. (2006). High-pressure structures and phase transformations in elemental metals. *Chem. Soc. Rev.* **35**, 943–963.
40. Bader R.F.W. (1990). *Atoms in Molecules. A Quantum Theory* (Oxford University Press, Oxford), 438 pp.
41. Edwards B., Ashcroft N.W. (1997). Spontaneous polarization in dense hydrogen. *Nature* **388**, 652–655.
42. Wells A.F. (1986). *Structural Inorganic Chemistry* (Clarendon Press, Oxford).
43. Hayami W. (1999). Theoretical study of the stability of  $\text{AB}_{12}$  (A = H-Ne) icosahedral clusters. *Phys. Rev.* **B60**, 1523–1526.
44. Werheit H., Luax M., Kuhlmann U. (1993). Interband and gap state related transitions in  $\beta$ -rhombohedral boron. *Phys. Status Solidi B* **176**, 415–432.
45. Tsgareishvili O.A., Chkhartishvili L.S., Gabunia D.L. (2009). Apparent low-frequency charge capacitance of semiconducting boron. *Semiconductors* **43**, 14–20.
46. Ma Y.M., Tse J.S., Klug D.D., Ahuja R. (2004). Electron-phonon coupling of  $\alpha$ -Ga boron. *Phys. Rev.* **B70**, 214107.
47. Brazhkin V.V., Taniguchi T., Akaishi M., Popova S.V. (2004). Fabrication of  $\beta$ -boron by chemical-reaction and melt-quenching methods at high pressures. *J. Mater. Res.* **19**, 1643–1648.
48. Le Godec Y., Kurakevych O.O., Munsch P., Garbarino G., Solozhenko V.L. (2009). Equation of state of orthorhombic boron,  $\gamma$ - $\text{B}_{28}$ . *Solid State Comm.*, **149**, 1356–1358.
49. Zarechnaya E.Y., Dubrovinsky L., Dubrovinskaia N., Filinchuk Y., Chernyshov D., Dmitriev V., Miyajima N., El Goresy A., Braun H.F., Vansmaalen S., Kantor I., Kantor A., Prakapenka V., Hanfland M., Mikhailushkin A.S., Abrikosov I.A., Simak S.I. (2009). Superhard semiconducting optically transparent high pressure phase of boron. *Phys. Rev. Lett.* **102**, 185501.
50. Zarechnaya E.Y., Dubrovinsky L., Dubrovinskaia N., Miyajima N., Filinchuk Y., Chernyshov D., Dmitriev V. (2008). Synthesis of an orthorhombic high pressure boron phase. *Sci. Tech. Adv. Mat.* **9**, 044209.
51. Jiang C., Lin Z., Zhang J., Zhao Y. (2009). First-principles prediction of mechanical properties of gamma-boron. *Appl. Phys. Lett.*, **94**, 191906.
52. Oganov A.R., Solozhenko V.L., Kurakevych O.O., Gatti C., Ma Y.M., Chen J., Liu Z., Hemley R.J. (2009). Comment on ‘Superhard Semiconducting Optically Transparent High Pressure Phase of Boron’. <http://arxiv.org/abs/0908.2126>.
53. Rulis P., Wang L., Ching W.Y. (2009). Prediction of  $\gamma$ - $\text{B}_{28}$  ELNES with comparison to  $\alpha$ - $\text{B}_{12}$ . *Phys. Stat. Sol. (RRL)* **3**, 133–135.